Finite Element Modeling for Flexible Pavement Behavior under Repeated Axle Load

Zainab M. Aljaleel
Civil Engineering Department, College of Engineering, University of Babylon, Iraq
zainab.ali.engh327@student.uobabylon.edu.iq (corresponding author)

Nahla Yasoub
Civil Engineering Department, College of Engineering, University of Babylon, Iraq
eng.nahlah.yassob@uobabylon.edu.iq

Yahya K. H. Atemimi
Civil Engineering Department, College of Engineering, University of Babylon, Iraq
eng.yahya.kadum@uobabylon.edu.iq

Received: 15 April 2024 | Revised: 2 May 2024 | Accepted: 15 May 2024

 DOI: https://doi.org/10.48084/etasr.7505

ABSTRACT

Accurate assessment of flexible pavement behavior requires a computational model that is able to predict the permanent deformation of the pavement under heavy load and its response with different thicknesses. This study developed several realistic models using advanced Finite Element Analysis (FEA) techniques employing the ABAQUS/CAE finite element program. The model integrates measured tire pavement contact stresses, moving wheel loads, and the viscoelastic properties of the asphalt layer. The model undergoes fine-tuning through the utilization of implicit dynamic analysis and variance in thickness. The simulations demonstrate that the viscoelastic behavior is more susceptible to changes in thickness. Furthermore, variation in thicknesses showed different pavement and rut depth behavior. The thinner the thickness is, the less resistance is applied to loading pressure and when the number of load repetitions increases, the depth of the rut also increases, leading to permanent deformation and consolidation with each passage of a heavy vehicle.

Keywords-rutting; viscoelastic theory; flexible pavement; FEM; load repetition

I. INTRODUCTION

A flexible pavement is a multi-layered structure designed to provide a surface for vehicle movement. Flexible pavements consist of several layers of materials. The asphalt layer, which is the initial layer of the pavement, is designed to withstand the maximum load. Beneath are the granular layers consisting of high-quality geomaterials, usually composed of coarse-grained unbound material. Ultimately, all loads are transmitted to the ground, which is made up of geotechnical materials. The pavement design consists of many parts and considers several factors, such as traffic volume, subgrade conditions, and environmental conditions. The ultimate performance of a complex system of layers is determined by the reaction of the materials within each layer to the dynamic forces exerted by the moving tire. Bituminous mixtures exhibit linear and viscoelastic behavior [1]. Current analytical procedures focus on the recoverable deformation of pavement layers, known as resilient behavior, while disregarding the non-recoverable absorbing behavior, when the deformation returns to what it was after the load is removed. This potentially leads to persistent rutting in the wheel path due to accumulated deformations during several load cycles. Therefore, recent studies [2, 3] have focused on developing viscoelastic or viscoelastoplastic models to represent the bituminous behavior materials. Repeated load and higher temperatures result in rutting, which is considered a crucial factor in evaluating the condition of the road exposed to high traffic loads [4, 5]. The difficulty associated with loading scenarios is the high number of load repetitions and the complex behavior of pavement layer materials contributing to the challenges of forecasting rutting in pavement. Therefore, a numerical model with efficient loading conditions and constitutive material models is required to accurately predict pavement rutting performance associated with loading cycles. Estimating the damage of heavy vehicles to the pavement following the Finite Element Method (FEM) is linked to the creation of a digital model that covers the properties of the material and the types of vehicles. Under a heavy vehicle load, FEM simulation calculates stresses and strains, as well as deflections that contribute to established pavement damage models that are developed mechanistically to estimate rutting [6]. The rutting is caused by the development of permanent distortion in the path of the wheel [7]. When pavement improvements were made, including increasing the

thickness of pavement layers, rutting was reduced, and this was confirmed in [8]. Deformations reduce the design life of the pavement and lead to increased maintenance and repair expenses [9]. According to [10] a pavement structure's response to loads includes stresses, strains, and deflections. Two important response points occur in the pavement structure, tensile strain below the bituminous layer, and compressive strain on the subgrade. Increasing compressive strain leads to the appearance of rutting [11].

This study aims to examine pavement layer behavior and rutting deformation, as well as the consequences of modifications in asphalt thickness in a multilayer pavement system, taking into account the viscoelastic behavior of asphalt.

II. CONSTITUTIVE MODEL USED IN MODELING

The most widely used approach to describe the constitutive behavior of pavement materials, known as the elastic theory, drastically underestimates how pavement would respond to vehicle loads. Furthermore, a recognized feature of asphalt, persistent deformation or delayed recovery, cannot be simulated by the elastic theory. It is not recommended to model asphalt as linear elastic, as this might cause premature failure of the pavement [3], [12]. Assuming that asphalt exhibits linear elastic behavior implies that each load applied will induce temporary deformation, which will be fully recovered upon load removal. In the context of pavement analysis, the linear theory presumes that small deformations are valid only for stress states. The two theories were analyzed by Abaqus program as portrayed in Figure 1 (a-c). The stress, strain and deflection when applying the viscoelastic theory increased significantly compared to the linear theory. In order to model the viscoelastic behavior of asphalt under different types of axle loads, the residual strain after the loading and unloading of the asphalt is reinserted during the analysis. In addition, asphalt's viscoelastic behavior is strongly influenced by temperature, and at higher temperatures, it becomes more viscous and prone to permanent deformation. A viscous material obeys Hook's law and Newtown's law, since the stress is dependent on the time rate of strain.

$$\sigma = \lambda \frac{\partial \epsilon}{\partial t} \quad (1)$$

where λ is viscosity and t is time. By integrating (1), it becomes:

$$\epsilon = \frac{\sigma_t}{\lambda} \quad (2)$$

Rutting can occur when a small amount of unrecoverable deformation (strain) accumulates from each load application.

III. FINITE ELEMENT MODEL FOR FLEXIBLE PAVEMENT UNDER HEAVY AXLE LOAD

Since flexible pavement can support varying axle loads and is affected differently by each type, it is important to understand the structural behavior of this material when it is subjected to external stresses. To simulate flexible pavement and estimate the behavior under heavy axle load, several models have been created, each model was subjected to axle load from a truck with different pavement layer thicknesses. As displayed in Figure 2, truck type 3-S3 was divided into several models.

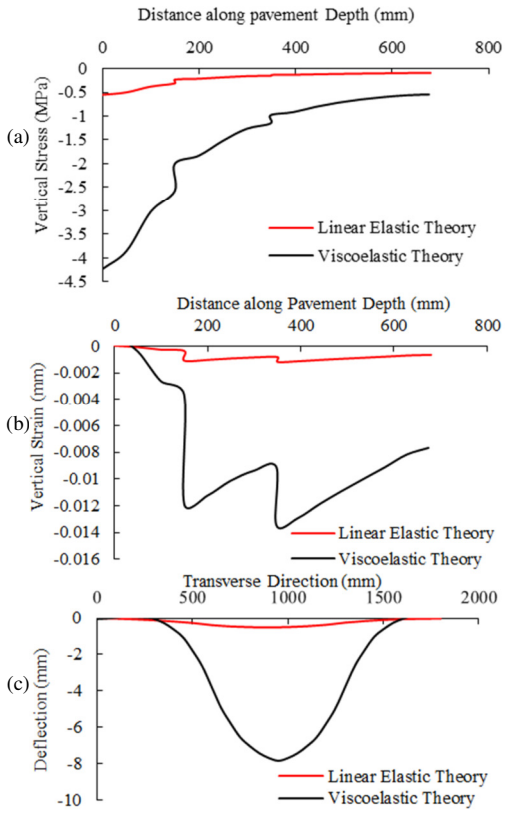

Fig. 1. Comparison of flexible pavement behavior with linear and viscoelastic theory for (a) stress, (b) strain, and (c) deflection.

A. Contact Area

When designing flexible pavements, the layered theory is applied and it is considered that all contact areas of tires are circular [13]. Instead of engaging two circular areas to depict a set of dual tires, using a single circle with the same contact area as the duals is a standard procedure, simplifying the examination of flexible pavements [14].

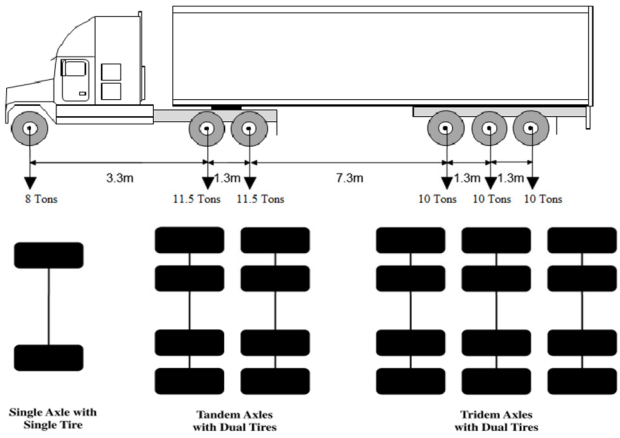

Fig. 2. Truck axles and tire configurations used in the models.

However, the semi-elliptical contact area of each tire can be represented by a rectangle combined with two semicircles, which is then converted into an equivalent rectangular area by using (3) and as evidenced in Figure 3.

$$C_A = \pi (0.3L)^2 + (0.4L)(0.6L) = 0.5227\, L^2$$

$$L = \sqrt{\frac{C_A}{0.5227}} \quad (3)$$

where C_A is the contact area of the tire with length L. The equivalent area is rectangular with dimensions of 0.8712L x 0.6L and the equal area $A = C_A = 0.5227\, L^2$. Table I presents the calculated results for the tire contact area and axle weight for a truck of type 3-S3.

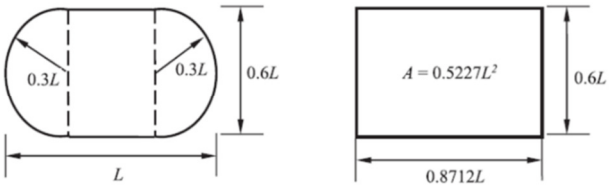

Fig. 3. Dimension of the tire contact area [15].

TABLE I. WHEEL LOAD INFORMATION.

Parameter	1st axle	2nd axle	3rd axle
Wheel configuration	Single	Dual	Dual
Number of wheels per axle	2	8	12
Axle weight (kN)	78	226	304
Length of equivalent area, 0.87L (cm).	35	35	35
Width of the equivalent area, 0.6L (cm)	25	25	25
Measured tire contact area, Ac (cm^2)	875	875	875
Contact pressure (MPa)	0.896	2.58	3.48

B. Load Type

Dynamic implicit analysis was employed for pavement simulation. Due to the movement of the vehicle wheels, the dynamic load occurs. They constantly change owing to irregularities in the pavement surface, vehicle speed, and weight. In dynamic implicit analysis, equations of motion are solved applying a time integration algorithm. The time latter considers the non-linear behavior of the material and the time-dependent loading. This allows for the simulation of complex dynamic phenomena, such as impact. The governing equation of a non-conservative dynamic system with material damping can be expressed using (4) [16, 17].

$$[M]\{\ddot{U}\} + [C] + \{\acute{U}\} + [K]\{U\} = \{P\} \quad (4)$$

here [M] is the mass matrix, [C] is the damping matrix, [K] is the stiffness matrix, {P} is the external force vector, {Ü}is the acceleration vector, {Ú}is the velocity vector, {U}is the displacement vector.

Flexible pavement is subjected to repeated loads from truck axles. In contrast changing the loading location gradually is necessary to enable full wheel rotation. The pavement model was divided into 12 increments to represent the path of a tire in an asphalt layer, to simulate the dynamic load on the pavement structure during testing. In addition, each step lies with a number of cycles. Repetition of the load was modeled deploying a time amplitude tabular, as noticed in Figure 4.

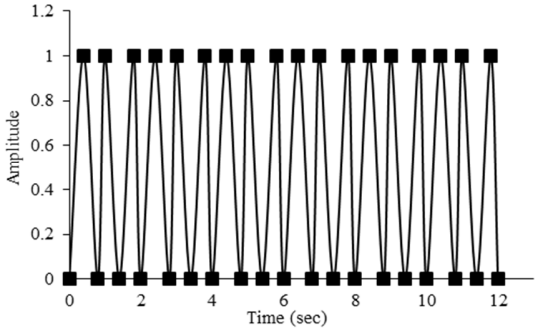

Fig. 4. Modeling repeated load by time amplitude.

C. Boundary Condition and Mesh Size

There is a difference between the boundary condition (BC) in statistical analysis and dynamic analysis. It is a general custom during dynamic analysis to define BCs to characterize the overall system behavior and to reduce the degree of freedom. The pavement model for the lateral sides tolerated a maximum political transversal displacement of 90 degrees. Thus, the two longitudinal displacements on the x-axis as well as the two displacements on the y-axis on the transverse sides were rigidly fixed at zero [18]. In addition, for the bottom (ENCASTER) BC where the deflection and rotation, which were restricted in all directions (U1=U2=U3=UR1=UR2=UR3=0) to avoid any horizontal or vertical movement of the bottom layer [19]. Figure 5 illustrates the load and boundary conditions utilized for the models and the longitudinal and transverse directions which represent the width and length of the pavement model of (3600 × 5000) mm, respectively.

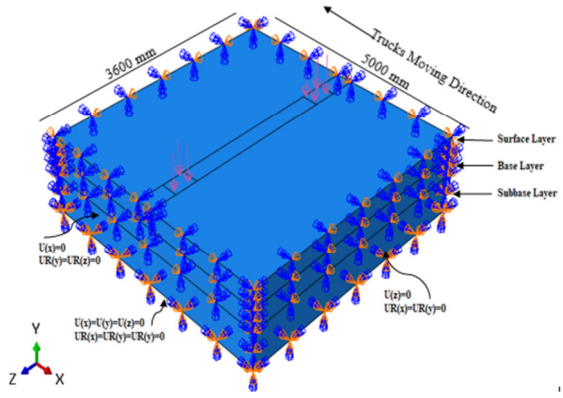

Fig. 5. Geometry and boundary condition of the models.

Mesh generation is an essential aspect of flexible pavement analysis deploying FEM. In the present study, and after a series of analyses, utilizing eight-node, linear brick elements, with reduced integration (C3D8R), with mesh size 50 mm. The total

numbers of elements and nodes are 203616 and 223380, respectively.

D. Flexible Pavement Thickness and Material Properties

To study the variation effect on the thickness of the flexible pavement, two cases of pavement thicknesses were considered, each including the layers depicted in Figure 6. The interaction between the layers is modeled by selecting the contact surfaces as "master" and "slave" roles. Pavement reactions to vehicle loads are greatly influenced by the contact conditions at the layer interfaces. The resistance to movement at the interfaces is often represented implementing the Coulomb friction model [20]. According to this model, the resistance at the interface is proportional to the typical stress. The interface prohibits movement up to a specific shear strength. Conversely, in the event of relative motion, the interfaces start to move towards each other. In this case, the frictional stress is constant [21].

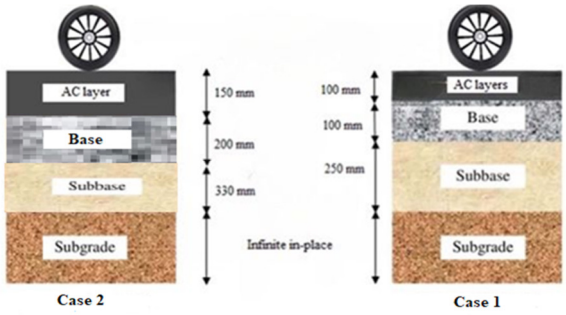

Fig. 6. Thickness of the pavement layers.

The properties of the materials considered for the pavement layers are summarized in Table II and include the modulus of elasticity (E), Poisson's ratio (v), density (g/cm3), and temperature (°C). These properties are crucial inputs in the Abaqus models to accurately represent the behavior of pavements under various loading conditions and environmental factors.

TABLE II. FLEXIBLE PAVEMENT LAYERS MATERIAL PROPERTIES.

Pavement layer	Elastic Modulus (MPa)	Poisson ratio (v)	Density (gm/cm^3)	Temperature (^oC)
Asphalt Concrete (AC)	2964	0.35	2.27	50
Base	2275	0.35	2.283	50
Subbase	110	0.3	2.24	50

IV. FINITE ELEMENT ANALYSIS RESULTS

One of the most important aspects this study focused on is the prediction of damage, especially in the depth of the rut and the estimation of the critical response points of flexible pavement layers under different heavy axle loads with multiple tire pressure and wheel configurations. These parameters include stress-strain and deflection in both substructures and superstructures. The relationship between pavement thickness and rut depth is an important factor in pavement design and maintenance, as detected in Figure 7. The results were extracted along the path of the wheel for the single axle, the tandem axle, and the tridem axle, considering a truck type 3-S3. The rut depth decreases from 6 to 4 mm, from 8 to 6 mm, and from 12 to 10 mm when pavement is subjected to single, tandem, and tridem axles respectively. This indicates that increasing the thickness of the flexible pavement results in a decrease in the depth of the rut. The percentage of rutting decreases is about 33%, 25%, and 17% when pavement is subjected to single, tandem, and tridem axles, respectively.

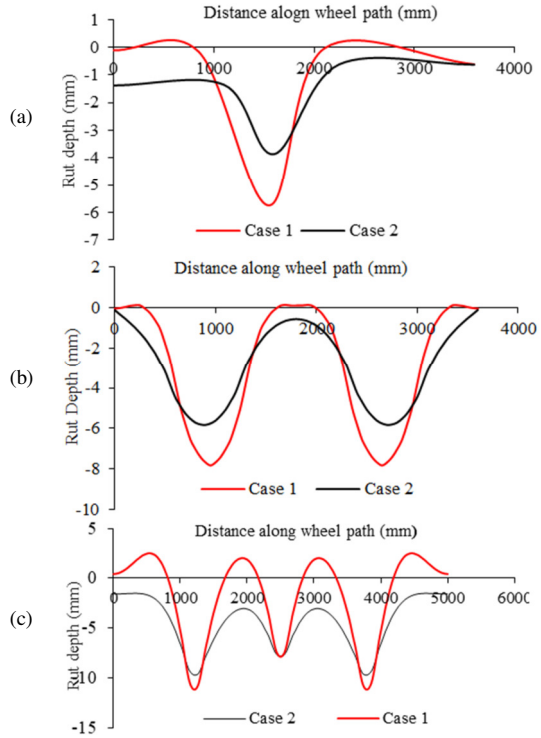

Fig. 7. Rut depth along the wheel path for (a) single axle single tire, (b) tandem axle double tire, (c) tridem axle dual tire.

Figure 7 (c) shows that the middle tire causes less deflection than the front and rear tires. This is because the middle tire is supported by the axle, whereas the front and rear tires are supported by the suspension. In addition, it explains the viscoelastic behavior of asphalt [2], as well as the distribution of loads on the sides, which is higher than the one on the middle, in contrast to a tandem load, where the first load cancels the second, and vice versa. This is explained more precisely by the simulation results in Figures 8-10. The x-axis stands for the transverse distance (mm), which represents the horizontal distance from the centerline of the tire to the point of measurement. The y-axis denotes the deflection (mm), which represents the vertical deflection of the pavement surface relative to its initial unrutted state.

Figures 8-10 showcase a cross section of the deformed shape of pavement under axle loads, taken from the center of wheel load. Pavement case 1 exhibited an increase in groove formation due to its lower load-bearing capacity, whereas pavement case 2 design experienced less grooving.

Understanding how stress and strain are distributed within a flexible pavement is important for pavement design. This is because excessive stress and strain can lead to premature

pavement failure. Flexible pavements with varying thicknesses display distinct stress and strain distributions due to the differential load bearing capacities and material properties of each layer [8]. On the other hand, the behavior depends on the relative abilities of the subsoil and the pavement to withstand deformation. The stress rate gradually decreases as it descends to the soil layers, and the lowest stress is in the last layer. Additionally, the variation in axle load under overloaded conditions represented by single, tandem and tridem axles contributes to the variation and distribution of stresses along the depths of the pavement as pinpointed in Figures 11 and 12.

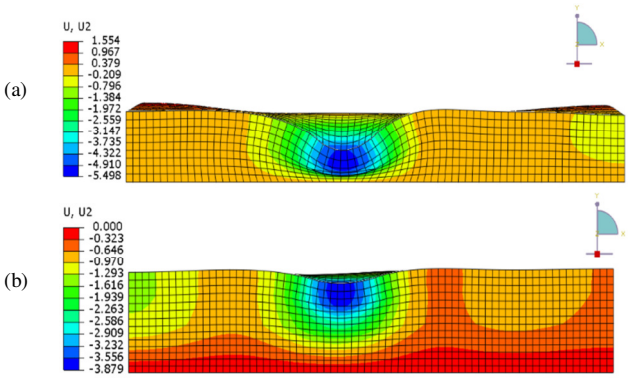

Fig. 8. Simulation results for rutting deformation of flexible pavement under single axle load for pavement (a) case 1, (b) case 2.

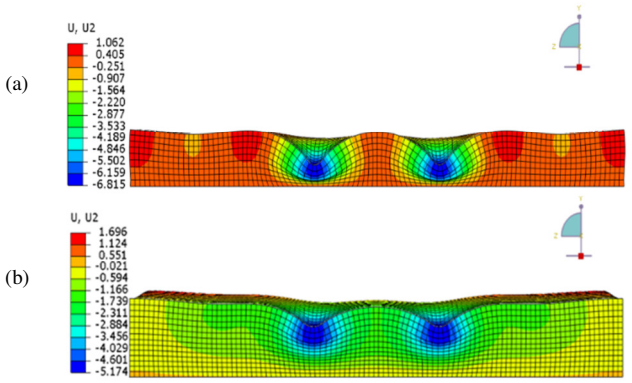

Fig. 9. Simulation results for rutting deformation of flexible pavement under tandem axle load for pavement (a) case 1, (b) case 2.

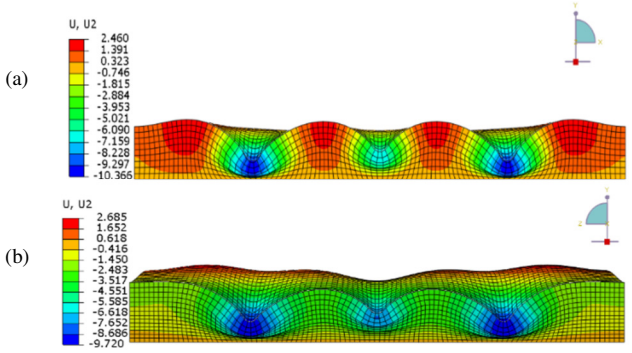

Fig. 10. Simulation results for rutting deformation of flexible pavement under tridem axle load for pavement (a) case 1, (b) case 2.

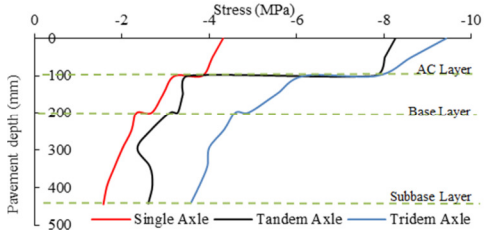

Fig. 11. Stress distribution along the depth of the pavement for pavement case 1.

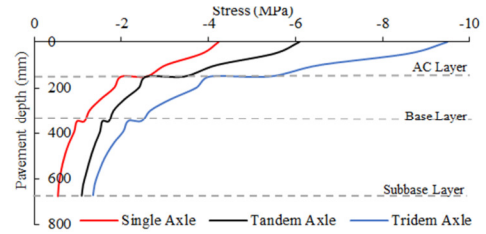

Fig. 12. Stress distribution along the depth of the pavement for pavement case 2.

Figures 11 and 12 demonstrate that stress gradually decreases as it propagates downward through the layers of a pavement. In contrast, similar fluctuation tendencies may be seen in the stress distribution throughout the pavement's depth under various axle loads. Conversely, the stress distribution in pavement case 2 reveals a significant difference compared to case 1, which has fewer thicknesses, with a marked decrease in the percentage of stress experienced by each axle type. The tridem axle exerts the greatest impact, followed by the decrease in the tandem axle, and the single axle experiences the least stress.

Figures 13 and 14 illustrate the strain along the depth of the pavement in case 1 and case 2.

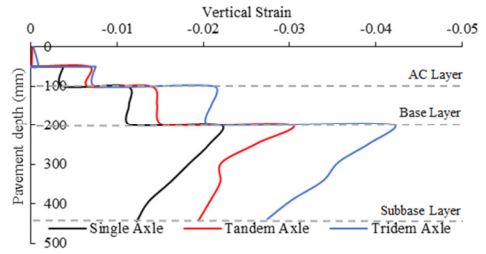

Fig. 13. Strain distribution along pavement depth for pavement case 1.

The strain in Figures 13 and 14 begins to increase until it reaches the highest level, when it reaches the bottom of the asphaltic layer and remains constant in the sub-base layer until it reaches the bottom of the layer. Even though at the sub-base layer, it begins to decrease, this variation in strain behavior is attributed to the different constitutive models and material properties of the pavement layer. In addition, the type of axle load also influences the strain distribution. Tridem axles induce the highest strains, followed by tandem axles, with single axles producing the lowest strains. This is due to the varying load intensities and contact areas of different axle configurations.

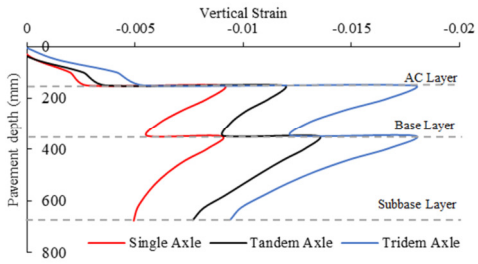

Fig. 14. Strain distribution along pavement depth for pavement case 2.

Asphaltic materials showcase time-dependent behavior particularly in response to load [22, 23]. The more repeated the axle load of the truck modeled (number of load repetition) is, the greater is the depth of the rut [4], leading to permanent deformation and consolidation with each passage of a heavy vehicle. Figure 15 indicates that despite the increase in the number of repetitions, the rutting decreased significantly with the augmentation in pavement thickness.

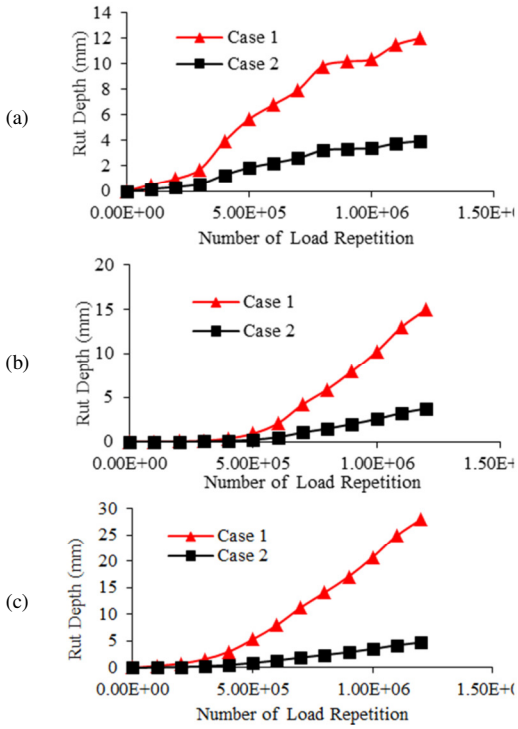

Fig. 15. Correlation between the depth of the rut and the number of repetitions of the load for the pavement of case 1 and case 2 under (a) a single axle (b) a tandem axle (c) a tridem axle.

The severity of rutting on asphalt concrete pavement is classified according to the average depth of the rut. According to the AASHTO 1993 classification [24], the severity levels are:

- Low: when the average depth of the rut is 6–13 mm.
- Medium: when the average depth of the rut is 13 to 25 mm.
- High: when the average rut depth is more than 25 mm.

V. CONCLUSIONS

In this study, different pavement thicknesses were modeled under different repeated axle loads to predict the rut depth of the flexible pavement and its response. The results disclosed that assuming that asphalt exhibits linear elastic behavior implies that each applied load will induce temporary deformation, which will be fully recovered upon load removal. The relationship between the rut depth and the number of load repetitions is linear. The rutting decreased significantly with the increase in pavement thickness and axle load.

REFERENCES

[1] Q. T. Nguyen, H. Di Benedetto, and C. Sauzéat, "Linear and nonlinear viscoelastic behaviour of bituminous mixtures," *Materials and Structures*, vol. 48, no. 7, pp. 2339–2351, Jul. 2015, https://doi.org/10.1617/s11527-014-0316-5.

[2] G. R. Chehab and Y. R. Kim, "Viscoelastoplastic Continuum Damage Model Application to Thermal Cracking of Asphalt Concrete," *Journal of Materials in Civil Engineering*, vol. 17, no. 4, pp. 384–392, Aug. 2005, https://doi.org/10.1061/(ASCE)0899-1561(2005)17:4(384).

[3] M. A. Elseifi, I. L. Al-Qadi, and P. J. Yoo, "Viscoelastic Modeling and Field Validation of Flexible Pavements," *Journal of Engineering Mechanics*, vol. 132, no. 2, pp. 172–178, Feb. 2006, https://doi.org/10.1061/(ASCE)0733-9399(2006)132:2(172).

[4] D. A. Saad and H. A. Al-Baghdadi, "Evaluation of Rutting in Conventional and Rubberized Asphalt Mixes Using Numerical Modeling Under Repeated Loads," *Engineering, Technology & Applied Science Research*, vol. 11, no. 6, pp. 7836–7840, Dec. 2021, https://doi.org/10.48084/etasr.4549.

[5] S. A. Tarawneh and M. Sarireh, "Causes of Cracks and Deterioration of Pavement on Highways in Jordan from Contractors' Perspective," *Civil and Environmental Research*, vol. 3, no. 10, pp. 16–26, 2013.

[6] M. Rahmani, Y.-R. Kim, Y.-B. Park, and J. S. Jung, "Mechanistic Analysis of Pavement Damage and Performance Prediction Based on Finite Element Modeling with Viscoelasticity and Fracture of Mixtures," *Land and Housing Review*, vol. 11, no. 2, pp. 95–104, 2020, https://doi.org/10.5804/LHIJ.2020.11.2.95.

[7] S. S. Almasoudi and A. H. K. Albayati, "Statistical Analysis of Component Deviation from Job Mix Formula in Hot Mix Asphalt," *Engineering, Technology & Applied Science Research*, vol. 12, no. 5, pp. 9295–9301, Oct. 2022, https://doi.org/10.48084/etasr.5225.

[8] M. M. Alamnie, E. Taddesse, and I. Hoff, "Advances in Permanent Deformation Modeling of Asphalt Concrete—A Review," *Materials*, vol. 15, no. 10, Jan. 2022, Art. no. 3480, https://doi.org/10.3390/ma15103480.

[9] G. A. Almashhadani and M. H. Al-Sherrawi, "Effect Change Concrete Slab Layer Thickness on Rigid Pavement," *Engineering, Technology & Applied Science Research*, vol. 12, no. 6, pp. 9661–9664, Dec. 2022, https://doi.org/10.48084/etasr.5283.

[10] Q. Li, D. X. Xiao, K. C. P. Wang, K. D. Hall, and Y. Qiu, "Mechanistic-empirical pavement design guide (MEPDG): a bird's-eye view," *Journal of Modern Transportation*, vol. 19, no. 2, pp. 114–133, 2011, https://doi.org/10.1007/BF03325749.

[11] M. Musbah, "Impact of Truck Overloading on Pavement Service Life (A Case in Awash-Mille Road)," Ph.D dissertation, Addis Ababa Science and Technology University, 2017.

[12] I. L. Al-Qadi and H. Wang, "Pavement Damage Due to Different Tire and Loading Configurations on Secondary Roads," Final report of NEXTRANS Project No 008IY01, 2009.

[13] D. Moazami and R. Muniandy, "Determination of rutting performance of asphalt pavements considering realistic tire-pavement contact area," *International Journal of Pavement Research and Technology*, vol. 14, no. 6, pp. 764–770, Nov. 2021, https://doi.org/10.1007/s42947-020-0187-9.

[14] E. J. Yoder and M. W. Witczak, *Principles of Pavement Design*, 2nd ed. New York: John Wiley & Sons, Ltd, 1975.

[15] Y. Y. Huang, *Pavement Analysis and Design*, 2nd ed. Pearson, 2003.

[16] K.-J. Bathe, *Finite Element Procedures in Engineering Analysis*. Prentice Hall, 1982.

[17] I.-W. Lee, D.-O. Kim, and G.-H. Jung, "Natural Frequency and Mode Shape Sensitivities of Damped Systems: Part I, Distinct Natural Frequencies," *Journal of Sound and Vibration*, vol. 223, no. 3, pp. 399–412, Jun. 1999, https://doi.org/10.1006/jsvi.1998.2129.

[18] O. C. Assogba, Y. Tan, X. Zhou, C. Zhang, and J. N. Anato, "Numerical investigation of the mechanical response of semi-rigid base asphalt pavement under traffic load and nonlinear temperature gradient effect," *Construction and Building Materials*, vol. 235, Feb. 2020, Art. no. 117406, https://doi.org/10.1016/j.conbuildmat.2019.117406.

[19] H. Taherkhani and M. Jalali, "Viscoelastic Analysis of Geogrid-Reinforced Asphaltic Pavement under Different Tire Configurations," *International Journal of Geomechanics*, vol. 18, no. 7, Jul. 2018, Art no. 04018060, https://doi.org/10.1061/(ASCE)GM.1943-5622.0001183.

[20] B. Park, S. Chun, and K. Kim, "Effect of various interface bonding conditions on critical response characteristics for cracking potential of asphalt pavements," *Road Materials and Pavement Design*, vol. 24, no. 8, pp. 2010–2026, Aug. 2023, https://doi.org/10.1080/14680629.2022.2117065.

[21] A. S. Romanoschi, "Characterization of Pavement Layer Interfaces.," Ph.D dissertion, Louisiana State University and Agricultural & Mechanical College, 1999.

[22] G. Qian, K. Hu, X. Gong, N. Li, and H. Yu, "Real-Time Flow Behavior of Hot Mix Asphalt (HMA) Compaction Based on Rheological Constitutive Theory," *Materials*, vol. 12, no. 10, Jan. 2019, Art. no. 1711, https://doi.org/10.3390/ma12101711.

[23] M. Lagos-Varas *et al.*, "Study of the mechanical behavior of asphalt mixtures using fractional rheology to model their viscoelasticity," *Construction and Building Materials*, vol. 200, pp. 124–134, Mar. 2019, https://doi.org/10.1016/j.conbuildmat.2018.12.073.

[24] "AASHTO Guide for Design of Pavement Structures." 1993.